

# We are IntechOpen, the world's leading publisher of Open Access books Built by scientists, for scientists

6,900

Open access books available

186,000

International authors and editors

200M

Downloads

Our authors are among the

154

Countries delivered to

TOP 1%

most cited scientists

12.2%

Contributors from top 500 universities



WEB OF SCIENCE™

Selection of our books indexed in the Book Citation Index  
in Web of Science™ Core Collection (BKCI)

Interested in publishing with us?  
Contact [book.department@intechopen.com](mailto:book.department@intechopen.com)

Numbers displayed above are based on latest data collected.  
For more information visit [www.intechopen.com](http://www.intechopen.com)



---

# Bio-Based Oil Drilling Fluid Improvements through Carbon-Based Nanoparticle Additives

---

Yee Ho Chai, Suzana Yusup, Vui Soon Chok and Sonny Irawan

Additional information is available at the end of the chapter

<http://dx.doi.org/10.5772/intechopen.74674>

---

## Abstract

Performance issues of vegetable oil or bio-based oil drilling fluids are generally inferior as compared to synthetic based drilling fluids. This chapter focuses largely on thermal conductivity and rheological properties of bio-based oil drilling fluid as its core issues. Unstable drilling fluids do not only incur in downtime for maintenance, but it indirectly affects production capacity as well. To overcome these issues, nanoparticles acts as additives to improve the thermo-physical traits of bio-based oil drilling fluid. The scope of this chapter focuses on dispersion of graphene oxide at very low concentration, namely 25, 50 and 100 ppm, to improve the thermal conductivity and rheological properties of bio-based oil drilling fluid. The data obtained from thermal conductivity and rheological experimental works were validated with various thermal conductivity and rheological models.

**Keywords:** bio-based oil drilling fluid, nanoparticles, thermal conductivity, rheology, graphene oxide

---

## 1. Introduction

Statistics have shown world energy consumption continues to experience growth rate since year 1990 with oil, natural gas and coal remaining as the major energy consumer [1]. Market report [2] has outlined increment in drilling activities and exploration as well as development of unconventional gas reserves will meet product's demands. The report also reported key players in the oil and gas industry to shift their focus in developing nanotechnology-based

solutions to overcome technological and environmental challenges. Asia Pacific was evaluated to have the highest market growth by 5.8% from 2016 to 2024 period [2].

Drilling fluids are highly regarded as one of the most important component in any drilling operations as it acts as a heat and solid circulating system, and a lubricant. It is reported that more than half of present global oil reserves stands at 4200 m below sea level at extreme temperature and pressure conditions [3]. However, extreme temperature and pressure conditions will cause drilling fluids to deteriorate. Deterioration in drilling fluids incurs downtime for maintenance and affects production capacity indirectly. Additives such as barite and bentonite are used to maintain density, rheology, temperature stability and fluid loss control properties of drilling fluids. However, this imposes several limitations including costly treatment cost and its inability to perform under HTHP conditions. For example, oil based muds have good lubricity properties, low torque and drag resistance [4] but performs poorly in terms of fluid loss circulation and elastomer compatibility [5], expensive and proved to be costly in terms of treatments and disposal of its cuttings. In addition, contaminated oil-based muds are often disposed to the surroundings, prompting environmental pollution to the surrounding seabed life and killing off coral reefs [6, 7]. Therefore, emphasis on drilling fluid containing biodegradable and environmental-friendly properties is inexorable for the preservation of marine environment.

The need to develop an environmental friendly drilling fluid system containing desirable attributes such as low toxicity, biodegradable and environmental friendly properties are highly demanded [8]. Some of the vegetable oils considered to be prospective base fluids are rapeseed oil, sunflower oil, palm oil and groundnut oil [5]. The ester composition within vegetable oils has intrinsic ability to biodegrade at the presence of "built-in" oxygen in esters [9]. However, esters contain high viscosity properties due to the presence hydrogen bonding of  $-OH$  groups in unsaturated fatty acids [5]. However, hydrogenation process is able to convert double bonds of unsaturated fats into saturated fats, thus altering the viscosity properties of vegetable oils to be less viscous. Vegetable oils such as *Jatropha* oil have higher flash point, better thermal stability and lower toxic compositions are advantageous over to diesel based muds [10]. Agwu et al. [11] had proven diesel oil to be chemically unstable in pour point and fire point analysis at extreme temperatures as compared to soybean oil. While chemical modifications such as hydrogenation process converts vegetable oils into less viscous states, it cannot be denied that oil-based fluids still possess low thermal conductance. To resolve such challenges faced by ester-based drilling fluids, incorporation and assimilation of nanotechnology into bio-based drilling fluids, such as nanoparticle additives, to be able to perform equally or better than the current conventional drilling fluids.

Nanofluids are binary systems [12] consisting of a base liquid suspended with metallic or non-metallic nanoparticles that acts as a colloidal suspension within the fluid with nanoparticles at average sizes of 100 nm or less [13]. Although nanofluids are often focused towards heat transfer applications, Choi [14] had proposed an important role for nanofluids for cooling and lubrication of drilling bits in future drilling operations. Nanoparticles are known to improve the rheological, mechanical and thermal properties of a given base fluid as they have higher specific surface areas, mechanical strengths and lower melting points [15]. Comparing

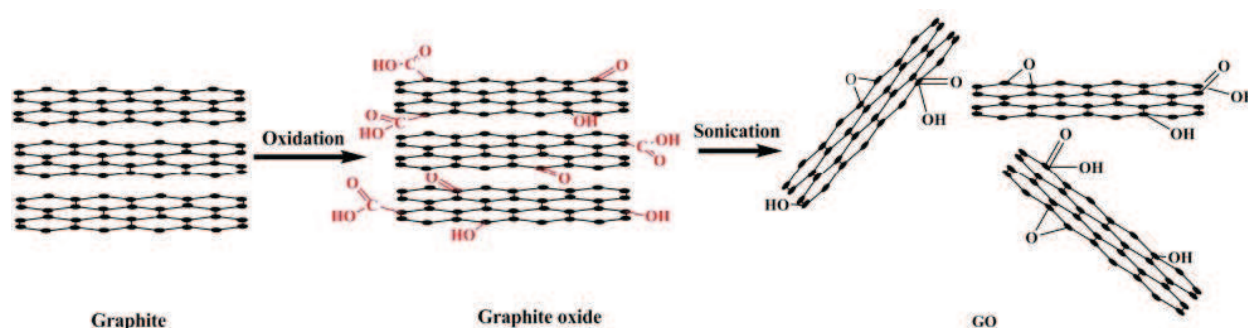


Figure 1. Schematic model of a graphene oxide sheet [18].

to micrometre and millimetre sized additives, nanomaterials also possess better dispersion stability, reduced pumping power [16] and clogging issues [17]. In general, oil-based drilling fluids are known to possess low thermal conductance, thus requiring nanoparticle additive to achieve better conductivity properties.

Graphene oxides are heterogeneous compounds which contain oxygen groups bonded to graphene sheets via oxidation process. Oxidized from graphite, graphite oxides readily exfoliate when undergoing ultrasonic process [18] as shown in **Figure 1**. Carbonyl and carboxyl groups are attached to the basal plane of graphene oxide [19]. Interestingly, graphene oxide possesses both soluble and non-soluble behaviours, which makes it versatile for production of nanofluids with a wide range of compatibility.

Presence of oxygen atoms can lead to alteration in vibrational characteristics of scattered phonons and subsequently reduce the free mean path [20]. The reduction of mean free path of phonons can lead to reduction in thermal conductivity properties. However, Mahanta and Abramson [21] suggested oxygen atoms paved interlayer interactions that induces higher phonon frequency and contributes to thermal conductivity increment. Functionalization of oxygen-groups on graphene sheets were used to enhance stability of nanoparticle suspensions in fluids through electrostatic stabilization from the media polarity [22].

## 2. Thermal conductivity and rheological properties

Thermal conductivity enhancement is influenced by several factors, such as Brownian motion of nanoparticles, nanolayer, nanoparticle clustering and other external parameters such as volume fraction, nanoparticle size and temperature [23]. Jang and Choi [24] discovered the random motion of Brownian motion contributed to 6% of total thermal conductivity enhancement. Nanolayers shown in **Figure 2** act as a barrier for thermal conductance which lowers the overall thermal conductivity of nanofluid. There are instances where clustering of nanoparticles by Van der Waals forces induces local percolation structure that can enhance thermal conductance of nanofluids [23].

However, a fractal model developed [25] showed no changes in thermal conductivity properties of nanofluid from clustering effects as the enhancement effects are counterbalanced from

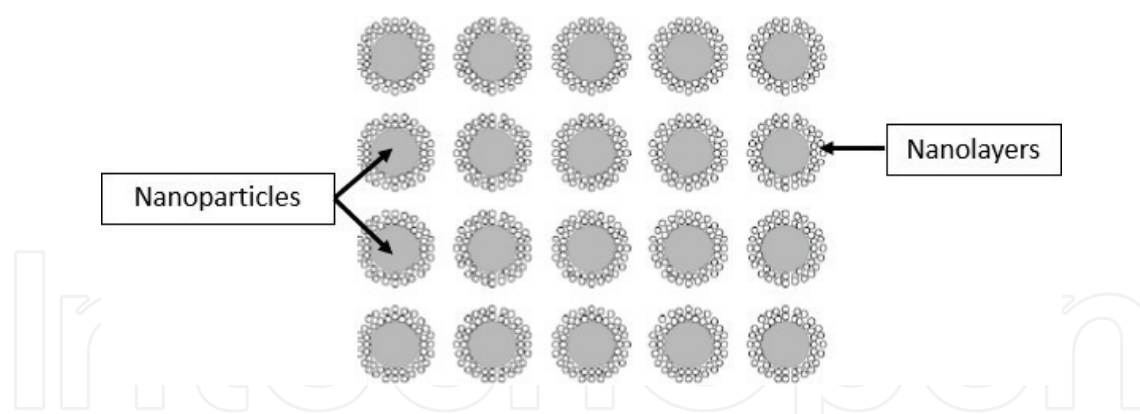


**Figure 2.** Schematic cross diagram of nanolayers at solid/liquid interface of nanoparticles and liquid [38].

reduced convection of particles. This claim was in good agreement that clustering effect performs poorly on stability and thermal conductivity of nanofluid [26].

Hadadian et al. [22] prepared different masses of graphene oxide in 50 mL of distilled water and ethylene glycol and were subjected to 15 min of ultrasonication to produce a homogeneous suspension. They yielded a maximum 30% thermal conductivity enhancement with 0.07 mass fraction graphene oxide, owing to the excellent geometry of graphene oxide such as high interfacial area and comprised of sheet-like arrangements favourable for formation of a percolation structure. Ijam et al. [27] added graphene oxide nanosheets ranging from 0.01 to 0.10 wt% into deionized water to be sonicated for 10 min before further diluted with ethylene glycol to obtain deionized water/ethylene glycol mixing ratio of 60:40. Their findings showed maximum thermal conductivity enhancement of 10.47% was obtained from maximum graphene oxide loading at 45°C in which they have highlighted the effects of sheet sizes to form a percolation pathway according to the percolation theory.

It is important to know the rheological behaviour of various types of fluids. The addition of nanoparticles into base fluids can alter the liquid's thermo-physical properties. Such enhancements are useful in heat transfer applications because of the high transfer enhancement in nanofluids. Therefore, the viscosity of fluid is greatly increased even at very low nanoparticle loadings [28]. Nevertheless, high viscosity properties enable solids such as drill cuttings to be suspended at stagnant conditions and prevents sagging process [29]. The trade-off for having high fluid viscosity incurs higher pumping costs of the fluid. Vajjha and Das [30] had proven nanoparticle concentrations greater than 3 vol% increases cost of pumping. Therefore, consideration for suitable nanoparticle selection should be taken into account for certain applications such as drilling purposes. Ijam et al. [27] compared shear stress and viscosity of graphene oxide-water nanofluids and concluded viscosity to function with respect to temperature. The increase in temperature weakens the intermolecular forces between particles to lower viscosity of nanofluids. Under high shear rate, viscosity of graphene oxide-water decreases exponentially until it reaches a point where it is independent of shear rate.

However, the rheological properties of nanofluids are still widely debatable among researchers. Fluctuating results were reported by various researchers stating addition of nanoparticles gives an increment or decrement of viscosity properties of nanofluids [31]. For example,

Wang et al. [32] dispersed graphene nanoparticles at low loadings into ionanofluid and was found to possess slightly lower viscosity at higher temperatures as compared to its counterpart base fluids due to the self-lubrication of graphene nanoparticles. Lu et al. [33] concluded rheological properties to be highly dependent on nanoparticle concentrations. At very low loadings, nanofluids with Newtonian behaviours can produce shear-thinning non-Newtonian behaviour when subjected to high nanoparticle concentrations due to strong particle-particle interactions interrupted by shear rates exceeding a specific critical value.

### 3. Thermal conductivity and rheological models

#### 3.1. Thermal conductivity models

Conventional thermal conductivity models are used for the prediction of thermal conductivity of nanofluids based on several main key parameters such as nanoparticle volume fraction ( $\phi$ ), thermal conductivity of nanoparticle ( $k_p$ ), thermal conductivity of base fluid ( $k_{bf}$ ) and shape factor ( $n$ ) for nanoparticle types. Effective medium theory (EMT) models, such as, Maxwell model [34], Hamilton-Crosser model [35] and Bruggeman model [36], are static models that predict based on the assumptions that particles are motionless and heat transfer between both continuous and dispersed phases are diffusive [37].

##### 3.1.1. Maxwell model

Maxwell had developed the first EMT model to predict suspensions containing diluted particles ( $< 1$  vol% concentration) [34]. The assumption basis of this model is that the particles are non-interacting with each other and is spherical in shape. Maxwell model is expressed as:

$$k_{nf} = \left[ \frac{k_p + 2k_{bf} + 2(k_p - k_{bf})\phi}{k_p + 2k_{bf} - 2(k_p - k_{bf})\phi} \right] k_{bf} \quad (1)$$

where  $k_{nf}$  is thermal conductivity of nanofluid,  $k_p$  is thermal conductivity of nanoparticle,  $k_{bf}$  is thermal conductivity of base fluid and  $\phi$  is the volume fraction of nanoparticle. The Maxwell model was reported to predict well for relatively large particle size at micro- and millimetre scales.

##### 3.1.2. Hamilton-Crosser model

The Hamilton-Crosser (HC) model is expressed when the thermal conductivity of particle is greater than the thermal conductivity of liquid by 100 times ( $k_p/k_{bf} > 100$ ). The HC model is an extension of Maxwell's model which takes shape factor,  $n$ , of particles into account in calculation. The shape factor is defined as the ratio of surface area of the sphere with constant volume as particle to the surface area of the particle.

$$k_{nf} = k_{bf} \left[ 1 + \frac{k_p + (n-1)k_{bf} + (n-1)(k_p - k_{bf})\phi}{k_p + (n-1)k_{bf} - (k_p - k_{bf})\phi} \right] \quad (2)$$

where  $n$  can be represented with  $n = 3/\psi$ ,  $\psi$  is the sphericity of the particle. Generally,  $n = 3$  is taken for spherical particles while  $n = 6$  is considered for cylindrical shape particles.

### 3.1.3. Bruggeman model

Unlike Maxwell model, Bruggeman model is applicable for two binary mixtures with no particle concentration limitations. However, Bruggeman model tends to deviate from Maxwell model at higher concentrations. The Bruggeman model is similar to that of Maxwell model as both models use the same assumption basis that the shape of particles are spherical. The Bruggeman model is written as follows:

$$\phi \left( \frac{k_p - k_{eff}}{k_p + 2k_{eff}} \right) + (1 - \phi) \left( \frac{k_p - k_{eff}}{k_p + 2k_{eff}} \right) = 0 \quad (3)$$

where  $\phi$  is the volume fraction of nanoparticles dispersed,  $k_{bf}$  is the thermal conductivity of base fluid,  $k_p$  as the thermal conductivity of nanoparticles and  $k_{eff}$  as the effective thermal conductivity of nanofluid.

## 3.2. Rheological models

Rheological models are used to determine the relationships between shear stress and shear rate as different applications possess different characteristics. Non-Newtonian models such as Bingham Plastic model [39] and Power Law model [40] are commonly used to predict rheological behaviours and are considered in this study.

### 3.2.1. Bingham Plastic model

Bingham Plastic fluids are unique as it has “infinite” viscosity until adequate stress is applied to initiate flow process. The Bingham Plastic model is as follows:

$$\sigma = \sigma_0 + \mu\gamma \quad (4)$$

where  $\sigma$  is the shear stress,  $\sigma_0$  is the limiting shear stress,  $\mu$  is the viscosity and  $\gamma$  is the shear rate. The limiting shear stress is often referred to as Bingham Yield Stress of the material. This model is suitable for concentrated mixtures and colloidal systems possessing Bingham behaviours.

### 3.2.2. Power Law model

Generally known as Ostwald model, non-Newtonian materials behave with respect to shear rate to produce two effects, namely shear thinning and shear thickening. Shear thinning yield lower viscosity when subjected to higher shear rate while shear thickening contradicts. The thickening is normally associated with the increase in sample volume and is known as dilatancy. The Power Law model is as follows:

$$\sigma = \mu \cdot \gamma^n \quad (5)$$

where  $\mu$  is the fluid viscosity,  $\sigma$  is the shear stress,  $\gamma$  is the shear rate and  $n$  is the power law index of the material. Shear thinning behaviour exhibits itself at  $n < 1$  while  $n > 1$  converts the material into a shear thickening fluid. This model is only limited to a small shear rate range as predictions from the model will deviate at a higher shear rate range.

## 4. Experimental study

### 4.1. Homogenization process

In this study, hydrogenated base oil (HBO) as base fluid and graphene oxide paste are supplied by a local company supplier. HBO is derived from vegetable oil through catalytic hydrotreating process and contains alkane chain branch between C15-C18. For the characterization of nanoparticles, graphene oxide paste was subjected to FTIR (Perkin Elmer) with wavenumber ranging from 500 to 4000  $\text{cm}^{-1}$  and TEM (Zeiss Libra 200FE) analysis at magnification range at 20,000x to 800,000x values. The HBO and graphene oxide paste were homogenized through a hydrodynamic cavitation unit at a constant flow rate of 1.5 L/min for 3 hours duration with an average of 10 bars pressure. The orifice diameter and length are 1 mm and 30 mm respectively. The schematic diagram is as shown in **Figure 3**. The hydrogenated oil-based nanofluids were transferred to an ultrasonic bath (Bath Ultrasonic Branson 8510E – DTH) for further homogenization.

### 4.2. Thermal conductivity properties analysis

Thermal conductivity analysis of hydrogenated oil-based nanofluids are carried out with KD2 Pro Thermal Properties Analyser equipped with KS-1 sensor with dimension

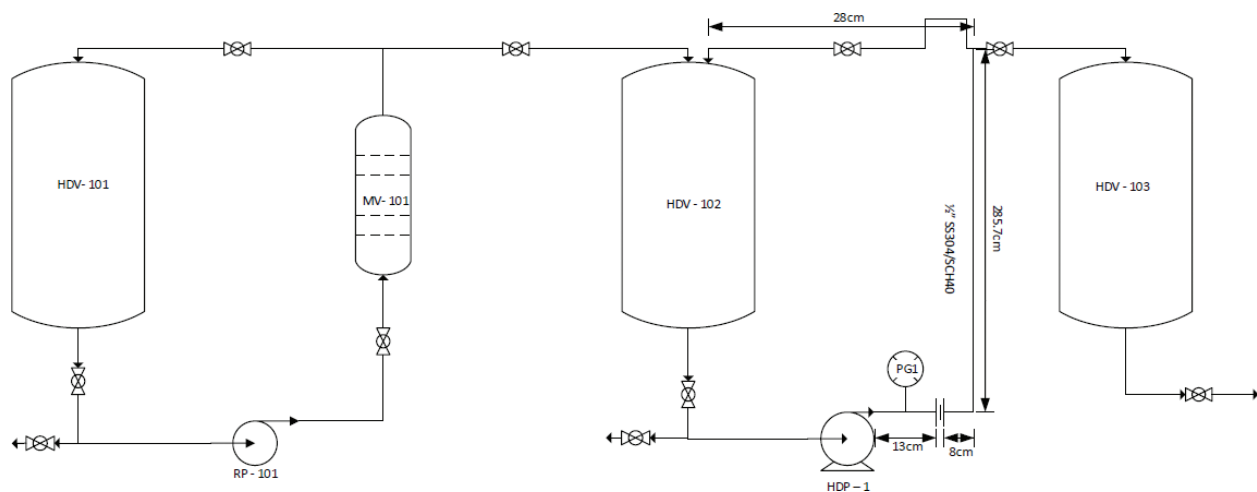


**Figure 3.** Schematic diagram of hydrodynamic cavitation unit (HDV: hydrodynamic vessel, MV: mixer vessel, PG: pressure gauge, RP: rotary pump, HDP: hydrodynamic pump).

1.3 mm diameter × 60 mm length) which complies with ASTM D5334-14 standards. The parametric studies in thermal conductivity analysis are divided into three categories, mainly the effect of temperature, the effect of nanoparticle concentrations and the effect of nanoparticle types. The temperature parameter in this study is set within the ranges of 30–50°C with a 5°C increase at each interval step. The presence of nanoparticles suspended within each sample move freely under elevated temperature, prompting fluctuations in thermal conductivity results. Therefore, each sample was repeated three times to ensure mean thermal conductivity is obtained. Further detailed explanation on the method can be found in our earlier work [48].

4.3. Rheological properties analysis

The parametric studies considered for the rheological properties analysis are viscosity values and shear stress values of hydrogenated base oil nanofluid with respect to shear rate and temperature. Rheological properties were measured using Malvern Bohlin Gemini II Rheometer following the method discussed in our earlier work [56].

5. Results and discussions

5.1. Characterization of graphene oxide

Tables 1 and 2 show the product specification of graphene oxide paste and vegetable oil by the local supplier respectively.

Carbon content (%)	>99.8
Oxygen content (%)	<0.05
Thermal conductance (W/m K)	2800
X-Y dimensions (μm)	0.06–1
Z dimensions (μm)	0.002–0.005

Table 1. Product specification of graphene oxide paste.

Parameters	Specifications
Density (kg/m <sup>3</sup> )	780 (at 15°C)
Initial boiling point (°C)	<300
Final boiling point (°C)	<330
Flash point (°C)	90
Kinematic viscosity (mm <sup>2</sup> /s)	2–2.6 (at 40°C)

Table 2. Product specification of hydrogenated oil-based fluid.

Two characterizations were used to characterize graphene oxide paste, namely FTIR analysis and TEM analysis. **Figures 4** and **5** show FTIR spectra analysis and TEM imaging of graphene oxide paste respectively.

At  $3500\text{ cm}^{-1}$  range, O-H group is present in graphene oxide as shown in **Figure 4** and is further supported by the findings of Farbod et al. [17]. Absorption peak between 1630 and

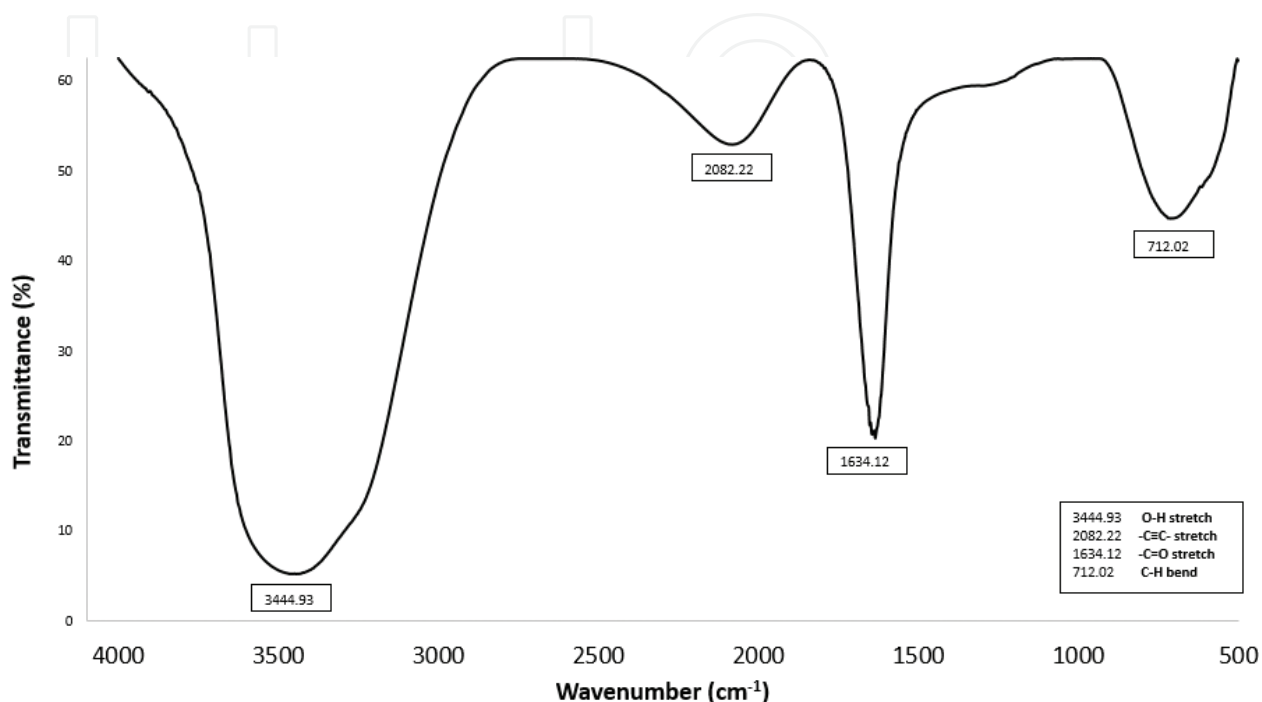


**Figure 4.** FTIR spectra analysis of graphene oxide.

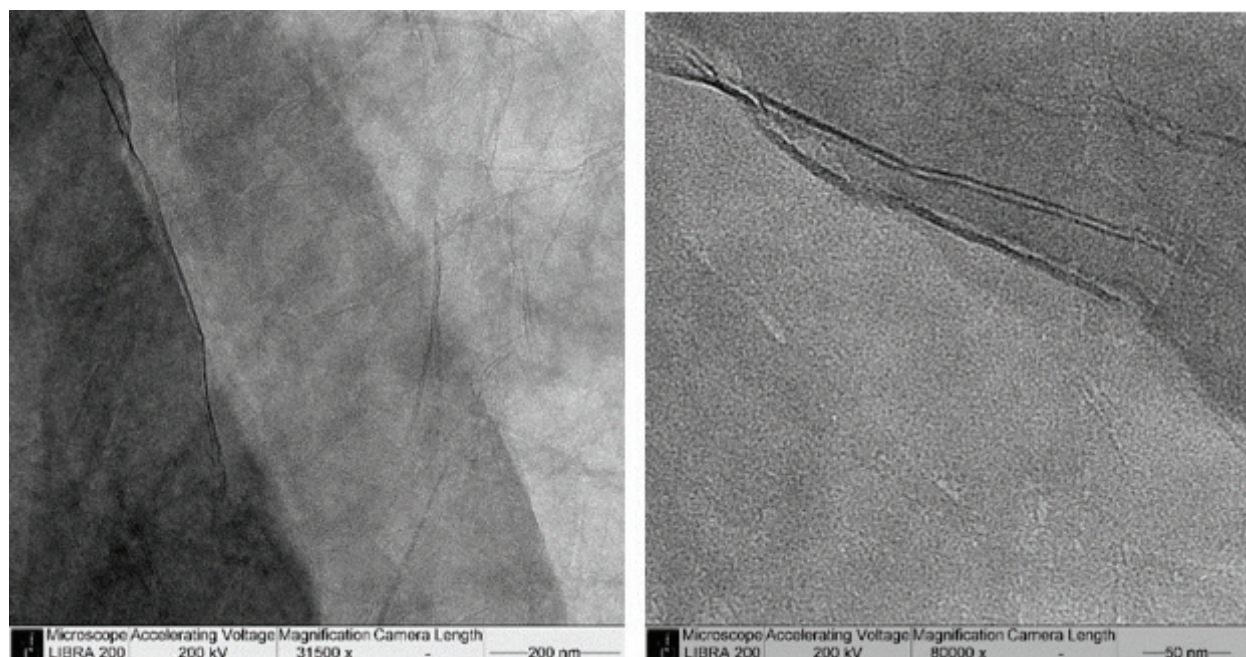


**Figure 5.** TEM image of graphene oxide at 31,500 $\times$  (left) and 80,000 $\times$  (right) magnifications.

1730  $\text{cm}^{-1}$  is assigned to C=O stretching of carboxylic and specific carbonyl functional groups [41]. The remaining peaks confirms the presence of carbon-carbon bonds which constitutes primarily from graphene sheets.

Stacking of graphene oxide sheets were outlined at 31,500 $\times$  magnification in **Figure 5** that shows folds and bends existing on the surface of graphene oxides. Schniepp et al. [42] explained that functionalized graphene sheets are distinctively different from graphene with the attachments of epoxy, hydroxyl and carboxyl groups on graphene sheets. The attachments of these groups posed lattice defects during thermal reduction process leading to the formation of defects on the surface of graphene oxides [42].

## 5.2. Thermal conductivity analysis

The effects of temperature and nanoparticle concentrations on thermal conductivity analysis was investigated. The analysis for graphene oxides dispersed in hydrogenated oil-based fluids were carried out at temperature of 30°C, 40°C and 50°C nanoparticle concentrations at 25 ppm, 50 ppm and 100 ppm.

Thermal conductivity of hydrogenated oil-based nanofluids as shown in **Figure 6** and **Table 3** increases linearly with temperature similar to the conclusions of other researchers [21, 43]. The increased in thermal conductivity values were regarded to the effects Brownian motion and micro-convection of nanoparticles induced by at higher temperature [19]. The influences of phonons, molecular diffusion and collision, and free electrons plays a vital role in this scenario [43]. Higher temperature provides better transfer of heat with regards to high phonon vibrations while intense molecular collisions enable better thermal conductivity between nanoparticles suspended.

Furthermore, **Figure 6** highlighted the dependency of thermal conductivity with respect to nanoparticle loadings. This trend is more apparent as high particle concentration contributes to higher collision between nanoparticles which prompted better diffusion and conductance of heat [43]. The same trend can be observed from the findings of other researchers [44]. Although thermal conductivity increment rate is apparent, it does not increase anomalously. The slight fluctuations in were attributed to the clustering of nanoparticles which prompted instability of the nanofluid suspensions. The choice of base fluid with low thermal conductance influences the suspension of nanoparticles into aggregates due to the immense intermolecular attraction force at a nanoscale at increasing concentration [45]. In **Figure 6**, 100 ppm showed lower thermal conductivity as compared to 25 ppm and 50 ppm concentration at 35°C onwards. This phenomenon is regarded to clustering of nanoparticles formed from high volume concentrations resulting in nanoparticle instability in the nanofluid. Agglomerations can provide local heat percolations that improves thermal conductivity [23] at sufficient higher energy input as shown at 50°C, however, the tendency of nanoparticles clustering that leads to settling of aggregates due to lower energy input into the system will result in reduced overall thermal conductivity enhancement. Furthermore, aggregations formed leads to larger variation in particle distribution and poses stability problems at higher temperature [45]. Hence, this could also be the contributing factor to the decrease in thermal conductivity

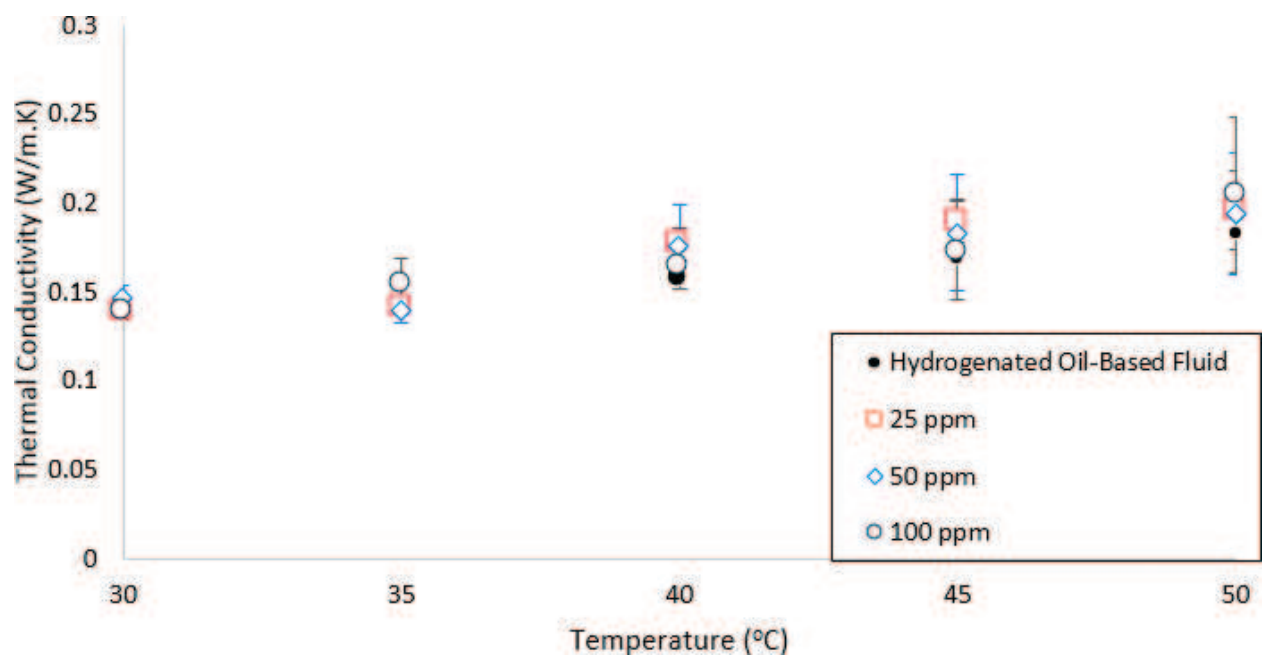


**Figure 6.** Thermal conductivity comparison of graphene oxide-hydrogenated oil nanofluid at 25 ppm, 50 ppm and 100 ppm.

Nanofluid type	Concentration (ppm)	Temperature (°C)	Mean thermal conductivity (W/mK)	Standard deviation (W/mK)
Graphene oxide–hydrogenated oil	25	30	0.1394	0.00518
		35	0.1408	0.00349
		40	0.1770	0.00914
		45	0.1898	0.01242
		50	0.1958	0.02191
	50	30	0.1464	0.00723
		35	0.1396	0.00659
		40	0.1753	0.02404
		45	0.1830	0.03290
		50	0.1940	0.03401
	100	30	0.1397	0.00437
		35	0.1543	0.01409
		40	0.1640	0.01284
		45	0.1736	0.02755
		50	0.2044	0.04361

**Table 3.** Thermal conductivity analysis of graphene oxide-hydrogenated oil based nanofluid with respect to different particle concentration and temperature.

performance at higher nanoparticle concentrations due to stability issues. Although presence of oxygen groups provides better stability and paved interlayer interactions [21] for improved thermal conductivity properties, the resulting shear pressure induced by hydrodynamic cavitation process have strained the structure of nanoparticle and in return, affects the stability of graphene oxide in this study.

The findings of this study are compared against our previous experimental work [46, 47] where graphene nanosheet and carbon nanotubes nanoparticles were selected. From **Figure 7**, graphene nanosheets have higher thermal conductivity as compared to carbon nanotube and graphene oxide by a slight margin at 50°C and 100 ppm. The high surface area to volume ratio and intrinsic thermal conductivity values of graphene nanosheets [48] contribute hugely to the increase in thermal conductivity of nanofluids at very low nanoparticle concentrations. Furthermore, larger sheet sizes attract one another and for conducting percolation pathway to conduct heat more efficiently [27], providing better thermal conductivity of graphene nanosheet and graphene oxide nanofluids as compared to carbon nanotube nanofluids.

A comparison between experimental data and the classical thermal conductivity models is shown in **Figure 8**. Similar to graphene nanosheets, graphene oxides are graphene sheets functionalized with oxide groups attached on the surface of the nanosheets. The Maxwell model is able to predict closely at 100 ppm as compared to lower particle concentrations. According to Gupta et al. [49], the contradictions between graphene nanosheets and graphene oxides is possibly influenced by different particle sizes. Gupta et al. [49] had compared the

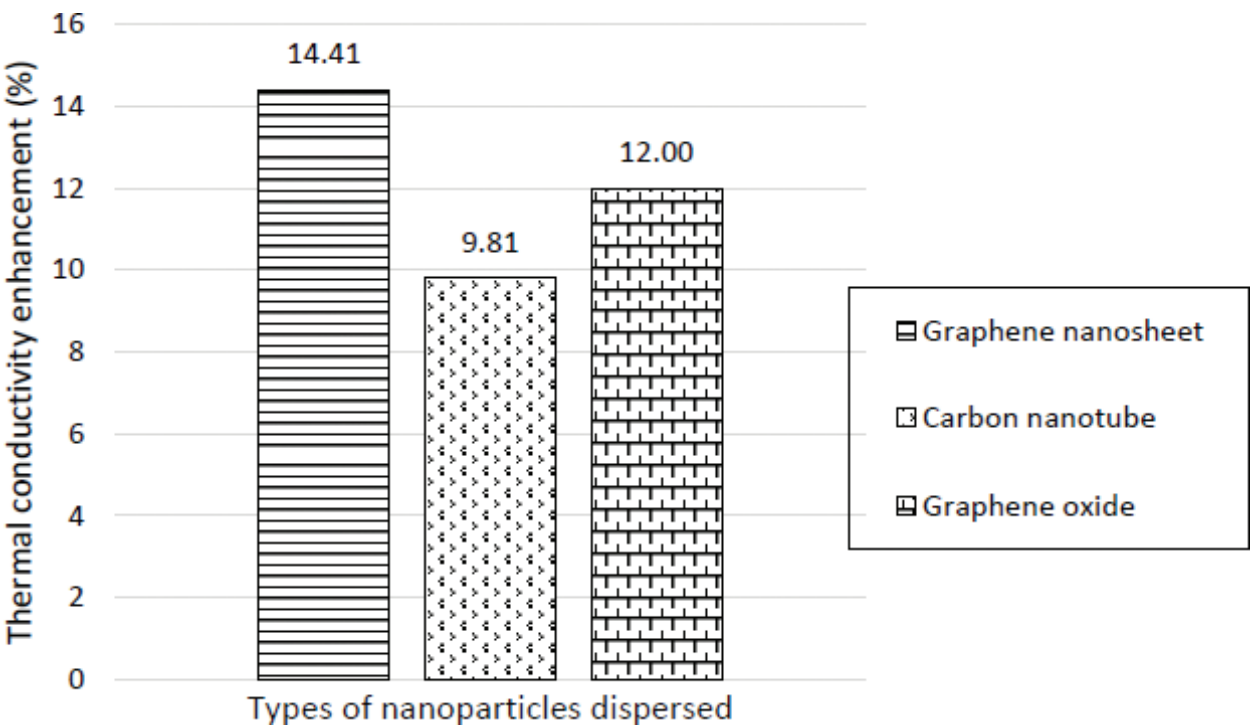


**Figure 7.** Thermal conductivity enhancement comparison between graphene nanosheets, carbon nanotubes and graphene oxide at 50°C and 100 ppm.

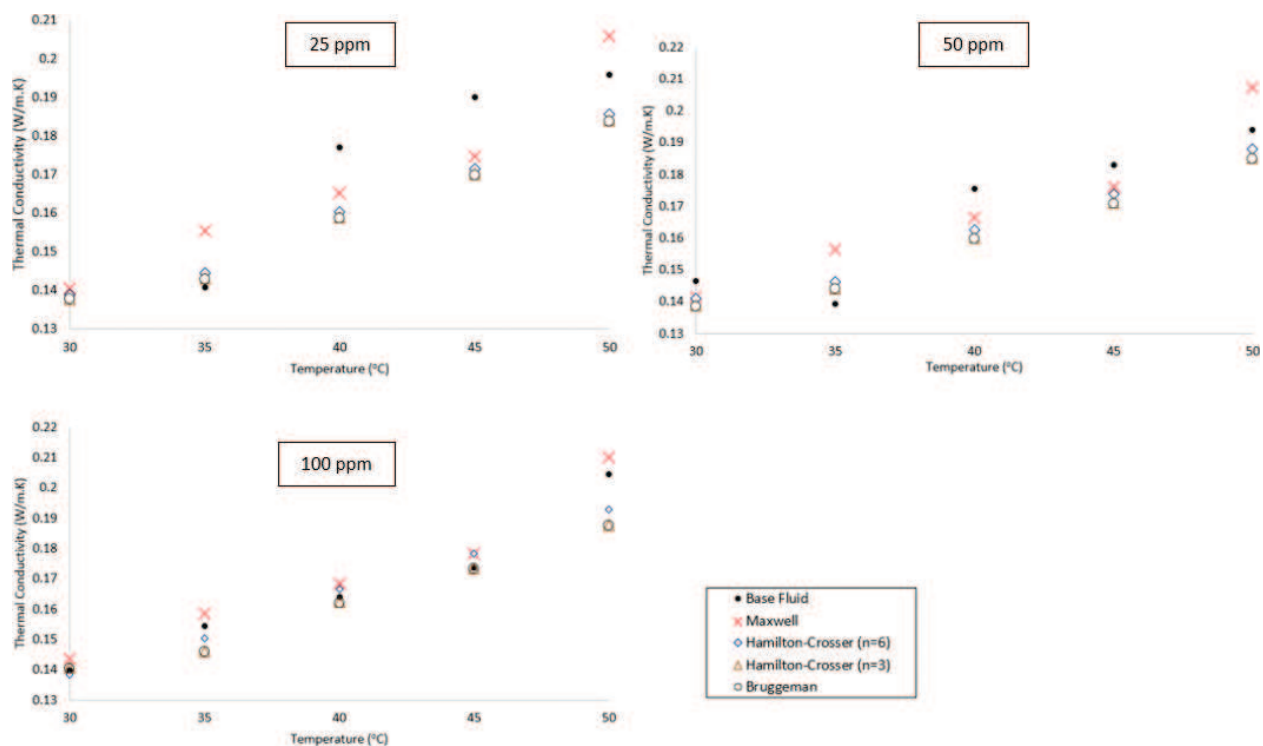


**Figure 8.** Comparison between experimental data and thermal conductivity models at 25, 50 and 100 ppm graphene oxide concentration.

sizes in their study and other researchers which lead to the conclusion of the role of particle sizes in the distribution and network formation for heat transfer. There have been various researches to improve Maxwell model with the inclusion of particle sizes [50] which can further improve the predictions of the models. In general, prediction of the models improved with respect to concentration, but consideration of higher nanoparticle concentrations should be modelled as well for a more accurate prediction by the models.

### 5.3. Rheological analysis

**Figure 9** shows the relationship of viscosity, shear rate and shear stress against the rheological behaviour of hydrogenated oil-based nanofluid. At low shear stress, Bingham fluids behave similar to a solid but flows in liquid manner when adequate stress is applied as shown in **Figure 9** (right) while Newtonian fluid will display constant viscosity regardless of the shear rate applied. From here, we can infer hydrogenated oil-based fluid to follow a non-Newtonian behaviour profile with a shear thinning behaviour.

**Figure 10** showed the comparison of viscosity profiles at 30°C, 40°C and 50°C with respect to increasing logarithmic shear rates and nanoparticle concentrations. The addition of graphene oxide does not influence the viscosity profile of pure hydrogenated oil-based fluid as shown in **Figure 9**. At higher shear rates, the viscosity of the nanofluids are closely similar at all concentrations with viscosity values overlapping each other.

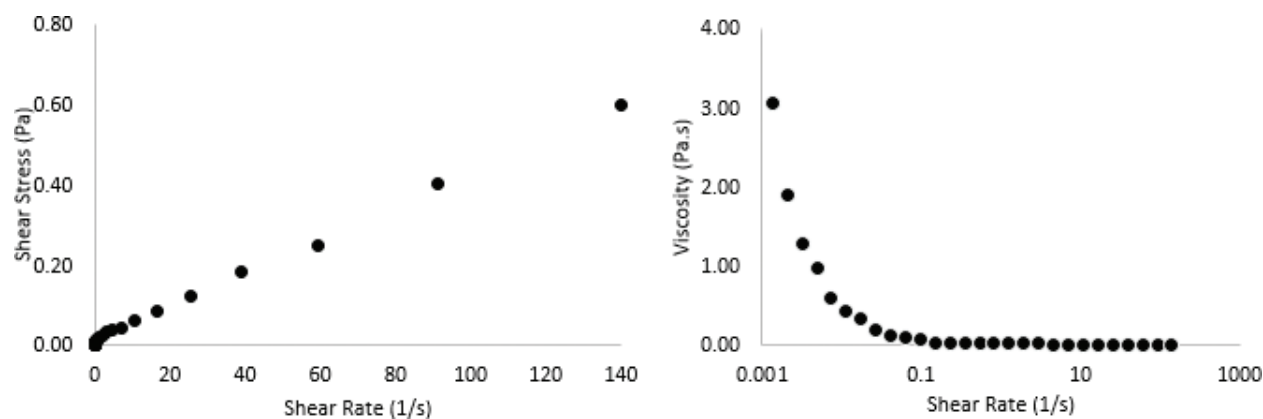


**Figure 9.** Graphical illustrations of shear stress (left) and viscosity (right) with respect to shear rate of hydrogenated oil-based fluid at 30°C.

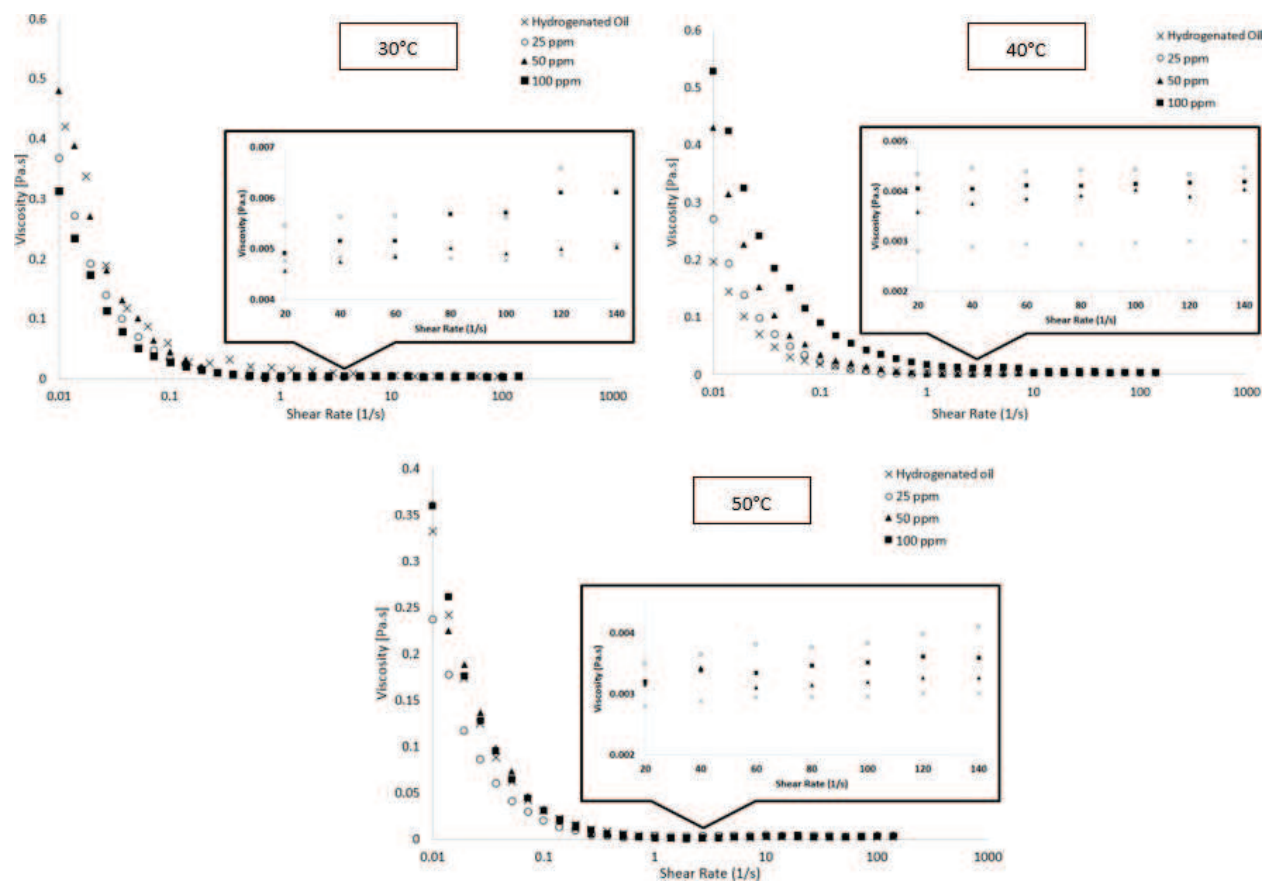


**Figure 10.** Comparison between viscosities at different concentration with respect to shear rate at 30°C, 40°C and 50°C.

At higher shear rate, the viscosity of nanofluids at various concentrations is seen decreasing exponentially towards the viscosity of the base fluid. However, upon closer inspection showed viscosity of hydrogenated oil-based nanofluids are higher compared to its base fluid counterpart. Similar to other studies carried out, the viscosity of nanofluids increases with higher concentrations but reduces when subjected to higher shear rates [51–52].

Interparticle frictions increase due to higher concentrations of nanoparticle suspended, thus highlighting the fluid's resistance to flow and subsequently increased the viscosity of nanofluids [43]. Furthermore, temperature parameter plays an important role in viscosity properties. Lower viscosity values are obtained at higher temperature and vice versa for constant nanoparticle concentrations due to the influence of temperature on the intermolecular attractions between nanoparticles and base fluid's particles. Interparticle and intermolecular adhesive forces of particles decreased at higher temperature because of higher energy input into the system [53], leading to the decrease of fluid's viscosity. This phenomenon was also observed by other researchers showing the effects of temperature against viscosity of nanofluids [19].

Two different behaviours of hydrogenated oil-based nanofluids can be deduced from this study, namely shear thinning and shear thickening behaviours. The nanofluids displayed shear thinning behaviour at lower shear rate while slight shear thickening behaviour was observed at higher shear rate instead due to percolation structure effects of nanoparticles suspension in base fluid [27, 54]. At high shearing rates, the formed percolation structure is broken down to form primary particles to form higher shear stress.

The rheological behaviour of hydrogenated oil-based nanofluids over the range of 30–50°C at concentrations 25 ppm, 50 ppm and 100 ppm were compared with non-Newtonian rheological

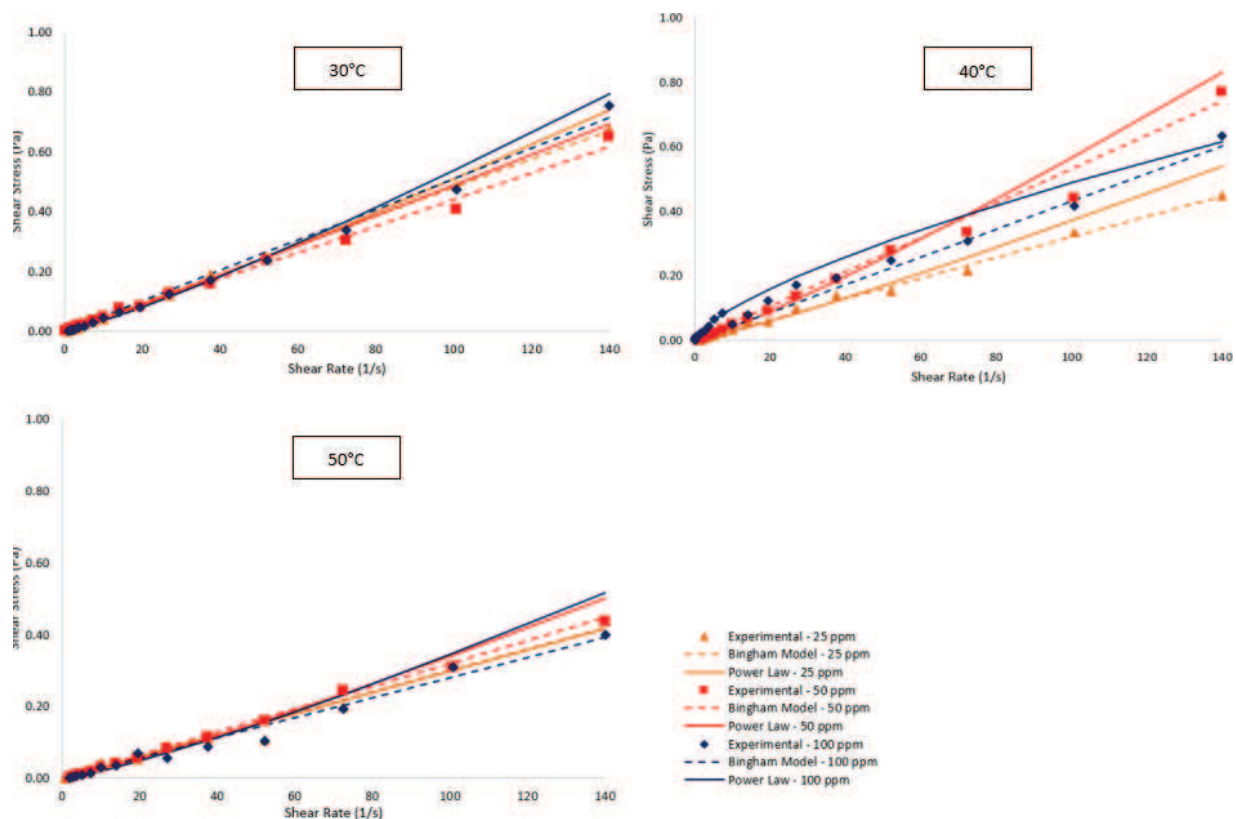


**Figure 11.** Comparison between experimental data and rheological models at different concentrations at 30°C, 40°C and 50°C.

models consisting of Bingham Plastic model and Power Law model as shown in **Figure 11** respectively. In **Figure 11**, it was observed 25 ppm concentration of graphene oxide dispersed yields the lowest shear stress while 50 ppm has the highest shear stress values at higher shear rates. A plausible explanation to this anomaly could be the increased stacking of graphene oxide sheets trapped due to the spindle's rotating movement. Comparisons have shown Bingham model gave better predictions of graphene oxide-hydrogenated oil-based nanofluids compared to Power Law model. The Power Law model over-predicted the shear stress values at higher shear rate due to the flow behaviour index at  $n > 1$ . Furthermore, hydrogenated oil-based nanofluid has comparatively similar yield stress values at different concentrations at higher temperatures. The rheological behaviour of hydrogenated oil-based nanofluids approaches a limit in which the shear stress values are independent to the concentration of nanoparticles at high temperature [55].

From the experimental analysis, hydrogenated oil-based fluid exhibits a non-Newtonian behaviour. Although the fluid exhibited zero shear stress at low temperature, the decreased in viscosity of hydrogenated oil-based fluid exhibited shear-thinning properties. However, the flocculation structure of nanoparticles was broken apart to form primary particle which led to slight shear thickening behaviour at higher shear rates. Similar to other findings, higher concentration of nanoparticles exhibits higher viscosity and shear stress properties but variations are insignificant upon comparison. Furthermore, the shear stress values are independent to the concentration of nanoparticles dispersed at higher temperature. The comparison between Bingham model and Power Law model showed Bingham model predicting better results data as compared to Power Law model at all concentrations, nanoparticle types and temperature.

## 6. Conclusion

In this study, graphene oxide-hydrogenated oil nanofluids were homogenized through combination of hydrodynamic cavitation and ultrasonication combination process at 25 ppm, 50 ppm and 100 ppm respectively. FTIR analysis had shown presence of large -OH groups concentration while TEM analysis shows severe defects and bends attributed to attachments of various groups on the surface. Findings have shown addition of graphene oxide into hydrogenated oil showed remarkable improvements of 12.00% in thermal conductivity enhancement at 100 ppm and 50°C. Furthermore, the rheological properties of hydrogenated oil nanofluid showed no significant changes in rheological behaviour when compared against the base fluid. Hydrogenated oil-based nanofluids have shown to possess both shear thinning and shear thickening behaviours at lower shear rates approaching higher shear rate range with increased viscosity at higher nanoparticle concentrations. Conventional thermal conductivity models were able to predict graphene oxide-based nanofluids accurately at higher particle concentration while Bingham Plastic model had shown to fit well against experimental data at all concentrations and temperature, thus proving addition of graphene oxide does not change the intrinsic behaviour of hydrogenated oil.

## Author details

Yee Ho Chai<sup>1</sup>, Suzana Yusup<sup>1\*</sup>, Vui Soon Chok<sup>2</sup> and Sonny Irawan<sup>3</sup>

\*Address all correspondence to: [drsuzana\\_yusuf@utp.edu.my](mailto:drsuzana_yusuf@utp.edu.my)

1 Chemical Engineering Department, Biomass Processing Laboratory, Centre for Biofuel and Biochemical Research, Institute for Sustainable Living, Universiti Teknologi PETRONAS, Perak, Malaysia

2 KL-Kepong Oleomas Sdn. Bhd, Selangor, Malaysia

3 Petroleum Engineering Department, Universiti Teknologi PETRONAS, Perak, Malaysia

## References

- [1] BP Statistical Review of World Energy 2016. London, UK. 2016
- [2] Grand View Research. Drilling Fluids Market Size to Reach \$12.55 Billion By 2024 [Internet]. [Updated: August 2017]. Available from: <http://www.grandviewresearch.com/press-release/global-drilling-fluids-market> [Accessed: June 2016]
- [3] Amani M, Al-Jubouri M, Shadravan A. Comparative study of using oil-based mud versus water-based mud in HPHT fields. *Advances in Petroleum Exploration and Development*. 2012;**4**(2). DOI: 10.3968/j.aped.1925543820120402.987
- [4] Udoh FD, Itah JJ, Okon AN. Formulation of synthetic-based drilling fluid using palm oil ester derived ester. *Asian Journal of Microbiology, Biotechnology and Environmental Sciences*. 2012;**14**(2)
- [5] Amarin R, Donsunmu A, Amankwah RK. Enhancing the stability of local vegetable oils (esters) for high geothermal drilling applications. *Journal of Petroleum and Gas Engineering*. 2015;**6**(8). DOI: 10.5897/JPGE2015.0215
- [6] Ismail A, Kamis A. Performance of the Mineral Blended Ester Oil-Based Drilling Fluid Systems. 12-14 June; Calgary. Calgary, Alberta: Petroleum Society of Canada; 2001. p. 4. DOI: 10.2118/2001-044
- [7] Al-Yasiri MS, Al-Sallami WT. How the drilling fluids can be made more efficient by using nanomaterials. *American Journal of Nano Research and Applications*. 2015;**3**(3):41-45. DOI: 10.11648/j.nano.20150303.12
- [8] Xie S, Jiang G, Chen M, Deng H, Liu G, Xu Y, et al. An environment friendly drilling fluid system. *Petroleum Exploration and Development*. 2011;**38**(3). DOI: 10.1016/S1876-3804(11)60040-2
- [9] Growcock FB, Patel AD. The Revolution in Non-Aqueous Drilling Fluids. April 12-14, 2011; Houston. Houston, Texas: American Association of Drilling Engineers; 2011

- [10] Paswan BK, Jain R, Sharma SK, Mahto V, Sharma V. Development of Jatropha in oil-in-water emulsion drilling mud system. *Journal of Petroleum Science and Engineering*. 2016;**144**:10-18. DOI: 10.1016/j.petrol.2016.03.002
- [11] Agwu OE, Okon AN, Udoh FD. A comparative study of diesel oil and soybean oil as oil-based drilling mud. *Journal of Petroleum Engineering*. 2015;**2015**:10. DOI: 10.1155/2015/828451
- [12] Yu W, Xie H. A review on nanofluids: Preparation, stability mechanisms, and applications. *Journal of Nanomaterials*. 2012;**2012**:17 <http://dx.doi.org/10.1155/2012/435873>
- [13] Mukherjee S, Paria S. Preparation and stability of nanofluids - A review. *Journal of Mechanical and Civil Engineering*. 2013;**9**(2):63-69. DOI: 10.9790/1684-0926369
- [14] Choi SUS. Nanofluids: From vision to reality through research. *Journal of Heat Transfer*. 2015;**131**(3):9. DOI: 10.1115/1.3056479
- [15] Moghaddam MB, Goshardi EK, Entezari MH, Nancarrow P. Preparation, characterization, and rheological properties of graphene-glycerol nanofluids. *Chemical Engineering Journal*. 2013;**231**:365-372. DOI: 10.1016/j.cej.2013.07.006
- [16] Saidur R, Leong KY, Mohammad HA. A review on applications and challenges of nanofluids. *Renewable and Sustainable Energy Reviews*. 2016;**15**(3):1-22. DOI: 10.1016/j.rser.2010.11.035
- [17] Farbod M, Ahanarpour A, Etemad SG. Stability and thermal conductivity of water-based carbon nanotube nanofluids. *Particuology*. 2015;**22**:59-65. DOI: 10.1016/j.partic.2014.07.005
- [18] Li J, Zeng X, Ren T, Heide EVD. The preparation of graphene oxide and its derivatives and their applications in bio-tribological systems. *Lubricants*. 2014;**2**(3):137-161. DOI: 10.3390/lubricants2030137
- [19] Hadadian M, Goshardi EK, Youssefi A. Electrical conductivity, thermal conductivity, and rheological properties of graphene oxide-based nanofluids. *Journal of Nanoparticle Research*. 2014;**16**:1-17. DOI: 10.1007/s11051-014-2788-1
- [20] Mu X, Wu X, Zhang T, Go DB, Luo T. Thermal transport in graphene oxide - From ballistic extreme to amorphous limit. *Scientific Reports*. 2014;**4**:9. DOI: 10.1038/srep03909
- [21] Mahanta NK, Abramson AR. Thermal Conductivity of Graphene and Graphene Oxide Nanoplatelets. 30 May-1 June 2012; San Diego, CA, USA. IEEE; 2012. p. 6. DOI: 10.1109/ITHERM.2012.6231405
- [22] Gudarzi MM. Colloidal stability of graphene oxide: Aggregation in two dimensions. *Langmuir*. 2016;**32**(20):5058-5068. DOI: 10.1021/acs.langmuir.6b01012
- [23] Aybar HŞ, Sharifpur M, Azizian MR, Mehrabi M, Meyer JP. A review of thermal conductivity models for nanofluids. *Heat Transfer Engineering*. 2015;**36**(13):1085-1110. DOI: 10.1080/01457632.2015.987586

- [24] Jang SP, Choi SUS. Role of Brownian motion in the enhanced thermal conductivity of nanofluids. *Applied Physics Letters*. 2004;**84**(21):4316-4318. DOI: 10.1063/1.1756684
- [25] Wu C, Cho TJ, Xi J, Lee D, Yang B, Zachariah MR. Effect of nanoparticle clustering on the effective thermal conductive of concentrated silica colloids. *Physical Review*. 2010;**81**:7. DOI: 10.1103/PhysRevE.81.011406
- [26] Murshed SS, de Castro C, Lourenço MJV. Effect of surfactant and nanoparticle clustering on thermal conductivity on aqueous nanofluids. *Journal of Nanofluids*. 2012;**1**(2):175-179. DOI: 10.1166/jon.2012.1020
- [27] Ijam A, Saidur R, Ganesan P, Golsheikh AM. Stability, thermo-physical properties, and electrical conductivity of graphene-oxide/deionized water/ethylene glycol based nanofluid. *International Journal of Heat and Mass Transfer*. 2015;**87**:92-103. DOI: 10.1016/j.ijheatmasstransfer.2015.02.060
- [28] Mishra PC, Mukherjee S, Nayak SK, Panda A. A brief review on viscosity of nanofluids. *International Nano Letters*. 2014;**4**(4):109-120. DOI: 10.1007/s40089-014-0126-3
- [29] Agarwal S, Phuoc TX, Soong Y, Martello D, Gupta RK. Nanoparticle-stabilised invert emulsion drilling fluids for deep-hole drilling of oil and gas. *The Canadian Journal of Chemical Engineering*. 2013;**91**(10):1641-1649. DOI: 10.1002/cjce.21768
- [30] Vajjha RS, Das DK. A review and analysis on influence of temperature and concentration of nanofluids on thermophysical properties, heat transfer and pumping power. *International Journal of Heat and Mass Transfer*. 2012;**55**(15-16):4063-4078. DOI: 10.1016/j.ijheatmasstransfer.2012.03.048
- [31] Ruan B, Jacobi AM. Ultrasonication effects on thermal and rheological properties of carbon nanotube suspensions. *Nanoscale Research Letters*. 2012;**7**(127):14. DOI: 10.1186/1556-276X-7-127
- [32] Wang F, Han L, Zhang Z, Shi J, Ma W. Surfactant-free ionic liquid-based nanofluids with remarkable thermal conductivity enhancement at very low loading of graphene. *Nanoscale Research Letters*. 2012;**7**(314):7. DOI: 10.1186/1556-276X-7-314
- [33] Lu G, Duan YY, Wang XD. Surface tension, viscosity, and rheology of water-based nanofluids: a microscopic interpretation on the molecular level. *Journal of Nanoparticle Research*. 2014;**16**(2564):11. DOI: 10.1007/s11051-014-2564-2
- [34] Maxwell J. *A Treatise on Electricity and Magnetism*. 1st ed. Oxford, UK: Clarendon Press; 1873. pp. 360-366
- [35] Hamilton R, Crosser O. Thermal conductivity of heterogeneous two-component systems. *Industrial & Engineering Chemistry Fundamentals*. 1962;**7**:187-191
- [36] Bruggeman D. Berechnung verschiedener physikalischer Konstanten von heterogenen Substanzen. I. Dielektrizitätskonstanten und Leitfähigkeiten der Mischkörper aus isotropen Substanzen. *Annals of Physics*. 1935;**416**(7):636-664

- [37] Lee JH, Lee SH, Choi CJ, Jang SP, Choi SUS. A review of thermal conductivity data, mechanisms and models for nanofluids. *International Journal of Micro-Nano Scale Transport*. 2010;**1**(4):269-321. DOI: 10.1260/1759-3093.1.4.269
- [38] Yu W, Choi SUS. The role of interfacial layers in the enhanced thermal conductivity of nanofluids: A renovated Maxwell model. *Journal of Nanoparticle Research*. 2003;**5**(1-2): 167-171. DOI: 10.1023/A:1024438603801
- [39] Bingham E. *Fluidity and Plasticity*. New York: McGraw-Hill Book Co.; 1922
- [40] Skelland A. *Non-Newtonian Flow and Heat Transfer*. New York: John Wiley and Sons; 1967
- [41] Loryuenyong V, Totepvimarn K, Eimburanapravat P, Boonchompoo W, Buasri A. Preparation and characterization of reduced graphene oxide sheets via water-based exfoliation and reduction methods. *Advances in Material Science and Engineering*. 2013;**2013**:5. DOI: 10.1155/2013/923403
- [42] Schniepp HC, Kudin KN, Li JL, Prudhomme RK, Car R, Saville DA, et al. Bending properties of single functionalized graphene sheets probed by atomic force microscopy. *ACS Nano*. 2008;**2**(12):2577-2584. DOI: 10.1021/nm800457s
- [43] Ahammed N, Asirvathama LG, Titus J, Bose JR, Wongwises S. Measurement of thermal conductivity of graphene-water nanofluid at below and above ambient temperatures. *International Communications in Heat and Mass Transfer*. 2016;**70**:66-74. DOI: 10.1016/j.icheatmasstransfer.2015.11.002
- [44] Keblinski P, Phillpot S, Choi SUS, Eastman J. Mechanisms of heat flow in suspensions of nano-sized particles (nanofluids). *International Journal of Heat and Mass Transfer*. 2002;**45**(4):855-863. DOI: 10.1016/S0017-9310(01)00175-2
- [45] Li CC, Hau NY, Wang Y, Soh AK, Feng SP. Temperature-dependent effect of percolation and Brownian motion on the thermal conductivity of TiO<sub>2</sub>-ethanol nanofluids. *Physical Chemistry Chemical Physics*. 2016;**18**:15363-15368. DOI: 10.1039/C6CP00500D
- [46] Chai YH, Yusup S, Chok VS, Arpin MT, Irawan S. Investigation of thermal conductivity of multi walled carbon nanotube dispersed in hydrogenated oil based drilling fluids. *Applied Thermal Engineering*. 2016;**107**:1019-1025. DOI: 10.1016/j.applthermaleng.2016.07.017
- [47] Chai YH, Yusup S, Chok VS, Arpin MT, Irawan S. Thermophysical properties of graphene nanosheets-hydrogenated oil based nanofluid for drilling fluid improvements. *Applied Thermal Engineering*. 2017;**122**:794-805. DOI: 10.1016/j.applthermaleng.2017.05.012
- [48] Ma W, Yang F, Shi J, Wang F, Zhang Z, Wang S. Silicone based nanofluids containing functionalized graphene nanosheets. *Colloids and Surfaces A: Physicochemical and Engineering Aspects*. 2013;**431**:120-126. DOI: 10.1016/j.colsurfa.2013.04.031

- [49] Gupta SS, Siva VM, Krishnan S, Sreeprasad T, Singh PK. Thermal conductivity enhancement of nanofluids containing graphene nanosheets. *Journal of Applied Physics*. 2011;**110**(8):6. DOI: 10.1063/1.3650456
- [50] Li FC, Yang JC, Zhou WW, He YR, Huang YM, Jiang BC. Experimental study on the characteristics of thermal conductivity and shear viscosity of viscoelastic-fluid based nanofluids containing multiwalled carbon nanotubes. *Thermochimica Acta*. 2013;**556**:47-53. DOI: 10.1016/j.tca.2013.01.023
- [51] Buongiorno J, Venerus DC, Prabhat N, McKrell T, Townsend J, Christianson R, et al. A benchmark study on the thermal conductivity of nanofluids. *Journal of Applied Physics*. 2009;**106**(9). DOI: 10.1063/1.3245330
- [52] Kole M, Dey TK. Investigation of thermal conductivity, viscosity, and electrical conductivity of graphene based nanofluids. *Journal of Applied Physics*. 2013;**113**(8):084307-01-084307-8. DOI: 10.1063/1.4793581
- [53] Thomas S, Sobhan CB. A review of experimental investigations on thermal phenomena in nanofluids. *Nanoscale Research Letters*. 2011;**6**(1):377. DOI: 10.1186/1556-276X-6-377
- [54] Kinloch IA, Roberts SA, Windle AH. A rheological study of concentrated aqueous nanotube dispersions. *Polymer*. 2002;**43**(26):7483-7491. DOI: 10.1016/S0032-3861(02)00664-X
- [55] Baratpour M, Karimipour A, Afrand M, Wongwises S. Effects of temperature and concentration on the viscosity of nanofluids made of single-wall carbon nanotubes in ethylene glycol. *International Communications in Heat and Mass Transfer*. 2016;**74**:108-113. DOI: 10.1016/j.icheatmasstransfer.2016.02.008
- [56] Chai YH, Yusup S, Chok VS, Arpin MT. Rheological behaviour of graphene nano-sheets in hydrogenated oil-based drilling fluid. *Procedia Engineering*. 2016;**148**:49-56. DOI: 10.1016/j.proeng.2016.06.490

IntechOpen

